NO. 21622

National Committee for Fluid Mechanics Films

FILM NOTES
for
RAREFIED GAS DYNAMICS*

By
F. C. HURLBUT and F. S. SHERMAN
University of California

Introduction

In the upper atmosphere and in many applications of vacuum technology, the average distance which a molecule travels between collisions with other molecules can become comparable to the characteristic dimensions of flight vehicles or vacuum chambers. When this happens, the qualitative characteristics of flow fields, and the appropriate conceptual framework for their analysis, depend upon the Knudsen number.

$$\mathrm{Kn} = \frac{\text{Molecular mean free path}}{\text{Characteristic length of body or chamber}} = \frac{\lambda}{d}$$

In the atmosphere, the mean free path increases from about 7×10^{-6} cm at sea level to about 80 meters at an elevation of 160 kilometers. The variation is roughly exponential with elevation.

In the film we show the evolution of a variety of flows as the Knudsen number assumes a wide range of values. These flows have greatly different appearances in the limits of very small and very large Knudsen number. Since the mechanics of collisions between gas molecules and solid surfaces assumes dominant importance when $\mathrm{Kn} >> 1$, we also show experiments which reveal important aspects of this "gas-solid interaction."

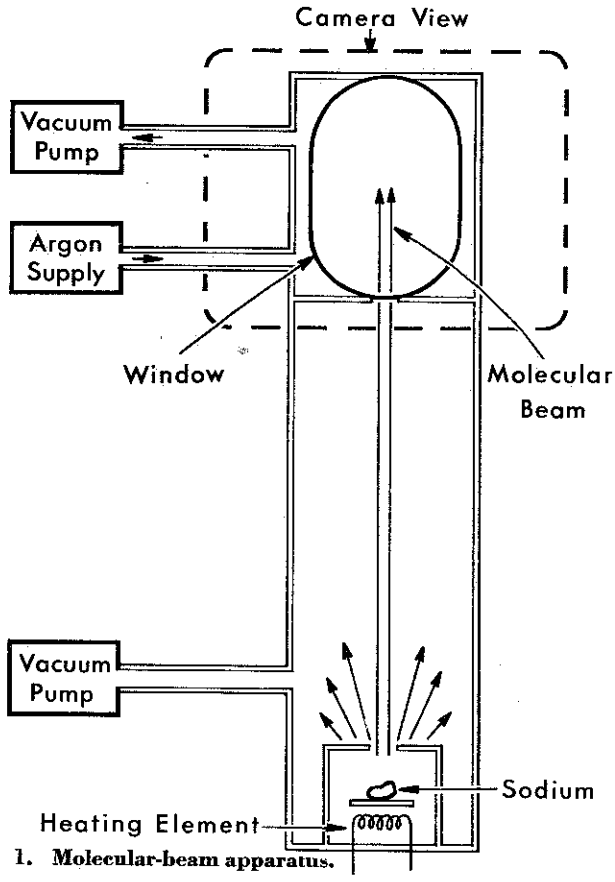

1. Molecular-beam apparatus.

** RAREFIED GAS DYNAMICS, a 16-mm black-and-white sound film, 33 minutes in length, was produced by Education Development Center under the direction of the National Committee for Fluid Mechanics Films, with the support of the National Science Foundation. Additional copies of the notes and information on purchase and rental of the film may be obtained from the distributor:*

Encyclopaedia Britannica Educational Corporation
425 North Michigan Avenue, Chicago, Illinois 60611
151 Bloor Street West, Toronto 5, Ontario

© 1970 Education Development Center

A Molecular Beam and Its Scattering By Collisions

Figure 1 shows an apparatus in which an initially well-collimated beam of sodium atoms travels through a chamber in which we can maintain a controllable density of argon. We observe the sodium beam, and its attenuation by collisions with the argon "background gas," as a function of argon density.

Sodium is evaporated in a small electrically-heated oven. A portion of the evaporated atoms emerge through an orifice, and some of these pass through the second orifice to form a fairly well-collimated molecular beam in the upper chamber. Both chambers can be pumped down to pressures below 10^{-5} torr (mm of Hg).

When a narrow sheet of light from a sodium discharge lamp is passed through the axis of the chambers, the sodium becomes visible because of a very efficient (resonant) light-scattering process.[1] The intensity of scattered light is proportional to the density of illuminated sodium atoms. The argon has a negligible scattering cross section for this light, and remains invisible.

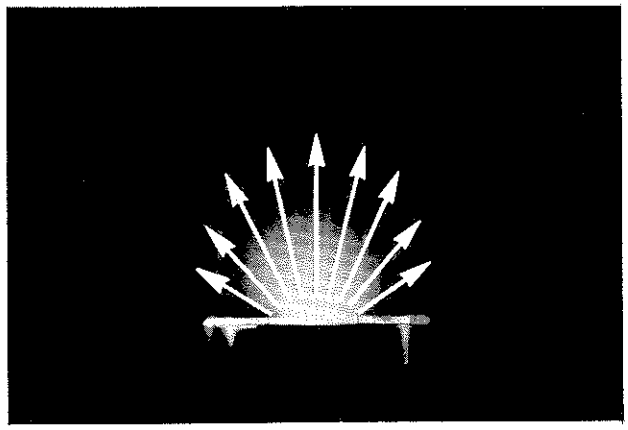

2. Illuminated sodium atoms in the emerging flow from the oven in the lower chamber.

Figure 2 is a scattered-light picture of the molecules effusing from the oven aperture. They move on straight-line paths away from the aperture, having a negligible number of collisions with other gas atoms at this low pressure. The mean free path is much longer than the interior dimensions of the chamber. Hence Kn $>>$ 1, and we say that a *free-molecule* flow is present.

Since the molecular paths diverge away from the aperture, the density decreases with distance from the gas source. However, with very fast film and long exposures,* we see the collimated sodium beam in the upper chamber. (Fig. 3a) The sharp edges of this beam indicate that the molecules do indeed follow straight lines between collisions.

*ASA 3000, 10-minute exposure

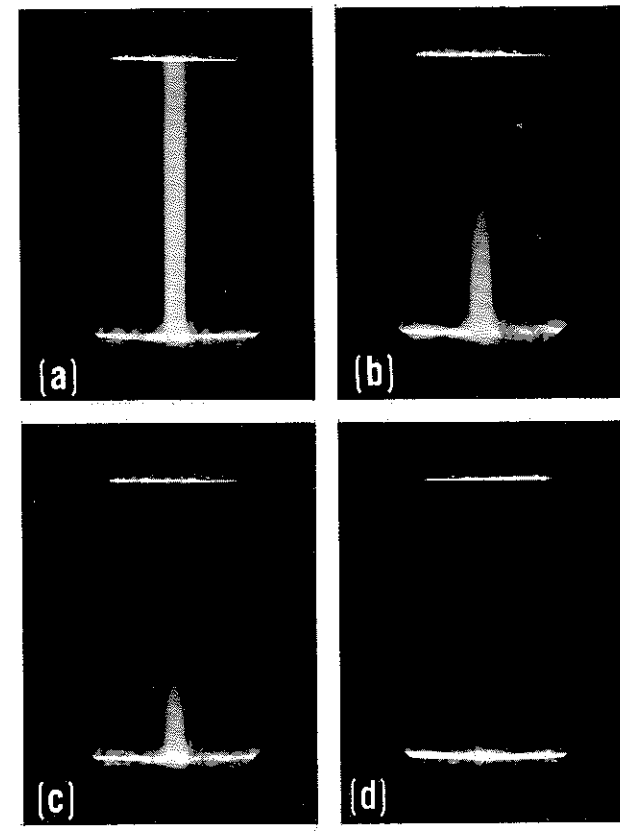

3. (a) Collimated sodium beam in the upper chamber. (b), (c), and (d) Increasing the density of argon in the chamber decreases the mean free path of the sodium atoms and reduces the visible penetration of the beam.

Next, argon is admitted to the upper chamber. As the density of argon is increased, the sodium beam fades out at the top (Fig. 3b), and becomes progressively shorter, (Figs. 3c and 3d). The mean free path of sodium atoms is inversely proportional to the density of the argon, and the visible penetration of the beam into the scattering chamber is roughly proportional to the sodium mean free path.

Collisions with the argon do not cause a diffused or fuzzy appearance of the sodium beam, because the scattered sodium atoms are dispersed into a very tenuous three-dimensional cloud, of which only a thin slice is illuminated.

When the sodium beam has virtually disappeared from the top chamber (Fig. 3d) the Knudsen number is very small. Sodium atoms still travel to the top of the chamber, but on often-interrupted and erratic paths, in a process which approaches ordinary diffusion.

Supersonic Flow Over a Blunt Body

The second experiment shows supersonic flow over a blunt body, with a 3000-fold variation of Knudsen number (Fig. 4).

A small washer is placed on the axis of a free jet of argon to which a trace of sodium vapor is added to

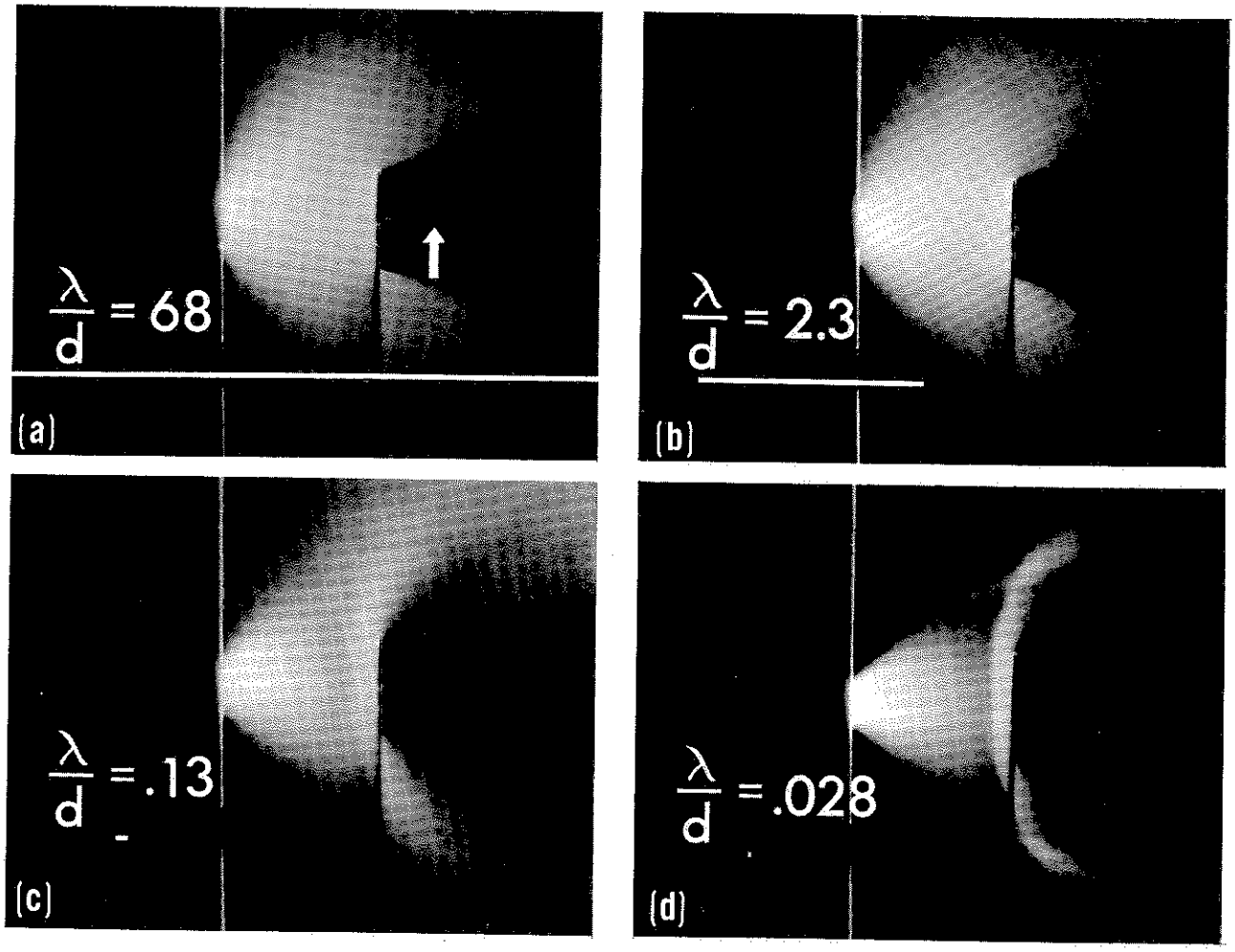

4. A washer in a free jet illustrates transition regimes between free-molecular and continuum flows. The characteristic dimension, d, in the Knudsen number is the diameter of the washer. The horizontal lines under the values of λ/d indicate the length of the mean free path, λ.* At the free-molecular extreme, the washer casts a sharp shadow and the hole forms a molecular beam. (See arrow.) (b) and (c) The shadow behind the washer becomes more diffuse and a compressed layer begins to form upstream. (d) At the continuum extreme, a bow shock wave is formed ahead of the washer.

allow flow visualization. The sodium light is introduced from above, in a thin sheet which passes through the axis of the jet. The washer is electrically heated to prevent condensation and collection of sodium. The purpose of the hole in the washer is to show what happens to molecules of the jet as they encounter molecules scattered back from the washer.

Figure 4a shows free-molecular flow for this configuration. By the time they reach the washer, molecules of the jet are traveling nearly straight away from the center of the jet-forming orifice. They pass right through the tenuous cloud of molecules scattered back by the washer, to define a sharp aerodynamic shadow in the wake of the washer. A well-collimated molecular beam emerges from the hole in the washer.

As the Knudsen number is decreased by increasing the rate of argon flow, the cloud of molecules scattered back by the model becomes dense enough to scatter molecules approaching the model. The flow through the hole in the washer loses its collimation and hence its visibility, and the aerodynamic shadow broadens. (Fig. 4b)

Further decreases in the Knudsen number (Figs. 4c and 4d) lead gradually to the formation of a shock layer in front of the body, within which a molecule entering from upstream suffers many collisions with other molecules before eventually finding its way to the model surface, or directly into the wake via the hole or around the outer perimeter of the model.

In Fig. 4d we see, with Kn $<<$ 1, a familiar hypersonic continuum flow. The Mach number at the model location is about nine. Further decrease in Knudsen number would make little noticeable change, except in the wake.

*The mean free paths represented by lines on the film are calculated from the formula

$$\lambda = \frac{1}{\sqrt{2}\, n\, \sigma^2}$$

The number density, n, is taken at the value which would be found on the jet centerline where the washer is located, if there were no washer. The collision cross-section used is $\sigma^2 = 36.5 \times 10^{-15}$ cm^2 (the viscosity cross-section of argon at the free-stream stagnation temperature). The sharp dark line below the washer is its optical shadow.

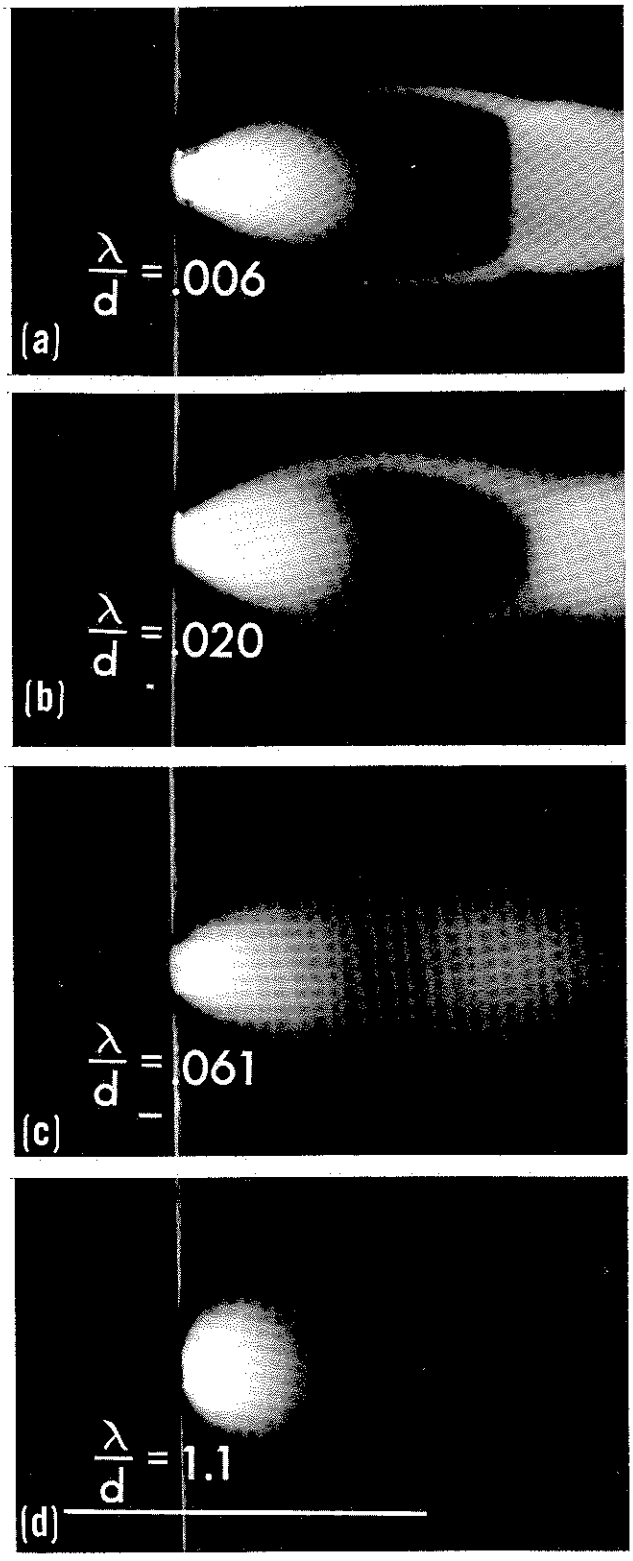

5. Transition from continuum to free molecular flow for the free jet alone. (a) At the continuum extreme a "barrel shock" exists from the nozzle exit to the "Mach disk." The characteristic dimension, *d*, is taken as the distance from the nozzle to the Mach disk for the continuum case. (b) and (c) Increase of mean free path causes shocks to become thick and diffuse. (d) At the free-molecular extreme, the shock system no longer exists. Further increase of the mean free path would not appreciably alter the flow.

Evolution of the Free Jet

The transition from continuum flow to free molecular flow from the same nozzle as in Fig. 4, but without the model, is shown in Fig. 5. With a small mean free path (Fig. 5a), the free jet gives rise to the familiar shock-wave pattern involving a barrel shock and a Mach disk. Similar patterns are often seen in rocket exhausts under appropriate continuum-flow conditions. These shock patterns are only clearly defined when the mean free path in the background gas is small compared to the distance from the nozzle to the Mach disk. Under these conditions the shock configuration depends only on the pressure ratio across the nozzle.

This pressure ratio is held constant at a hundred to one, and the results of increasing the mean free path by decreasing the argon flow are shown in Figs. 5b through 5d. When the mean free path is no longer negligible compared to the jet dimensions, the shocks become very thick and fuzzy (Fig. 5b). The barrel shocks spread out until they overlap and mix in with the Mach disk. In Fig. 5c, only a hazy, slightly bright spot remains to remind us of the shock system. In the free-molecule limit (Fig. 5d), the jet molecules no longer collide with the background molecules, but fly straight past them to the chamber walls. The background molecules, for their part, can fly right through the jet without collision.

Surface Interactions

To make quantitative predictions of aerodynamic forces or heat transfer in free-molecule flow, we must have at least some statistical knowledge of the outcome of collisions between gas molecules and solid surfaces.

A. *Sodium-Beam Experiment*

Figure 6 illustrates visually the important concept of diffuse reflection.

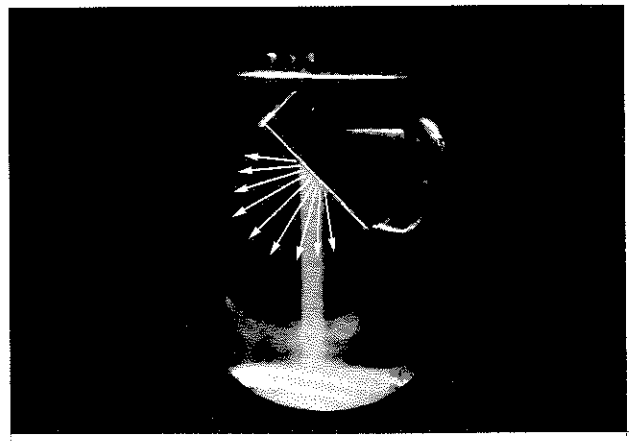

6. A polished aluminum oxide surface is positioned at 45° to the sodium molecular beam. The beam is not reflected as a light ray is from a mirror, but rather is scattered in all directions as the superposed arrows indicate. The density of the scattered molecules is too small to be recorded on the film.

A surface of polished aluminum oxide is mounted in the upper chamber of the sodium-beam apparatus, at an angle of 45° to the incident beam. The target is heated to the temperature of the beam oven, so that condensation of the sodium on the target is prevented.

Although the sodium beam appears to end at the target, the sodium atoms are actually re-emitted in every direction away from the spot of impact. Once again they are scattered into a cloud too tenuous to be seen. Clearly, the molecular beam is not reflected specularly from the target, as a light beam reflected from a mirror would be. More quantitative experiments confirm that nearly diffuse re-emission of molecules is typical at ordinary or even highly polished surfaces. However, highly directed scattering is sometimes observed, particularly when the surface is composed of atoms in a well-ordered array and is free of adsorbed gases.

B. *Momentum-Transfer Experiment*

The integrated effects of momentum transfer in gas-solid collisions can be studied directly by observing the torque exerted on a target surface subjected to the off-center impact of a molecular stream (Fig. 7). The

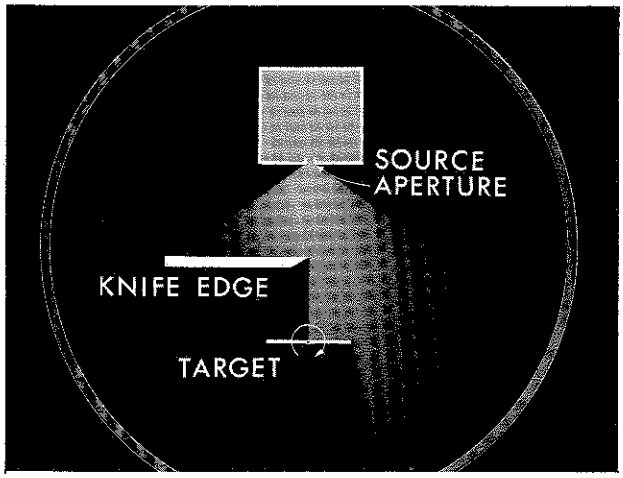

7. Plan view schematic of momentum-transfer experiment. A torque is applied about the center of suspension of the target.

apparatus consists of a gas source with slit aperture, a knife edge, and a target, all within a cylindrical glass vacuum chamber.

The target and a small mirror are attached to a vertical torsion wire. When enough gas is supplied to the source to produce a free-molecule effusion through the slit, the target is turned by the impact of molecules on its unsheltered half. A light beam reflects from the mirror to record the angle of target deflection on a large index circle.

The experiment is begun by indexing the light spot with the target oriented as shown in Fig. 7. Gas is admitted to the source, and source pressure and target deflection are noted. The top of the torsion wire is then twisted to return the target to its initial position. The source pressure is doubled, and the new deflection noted. Figure 8 shows typical data of the torque required to hold the target in the position of Fig. 7,

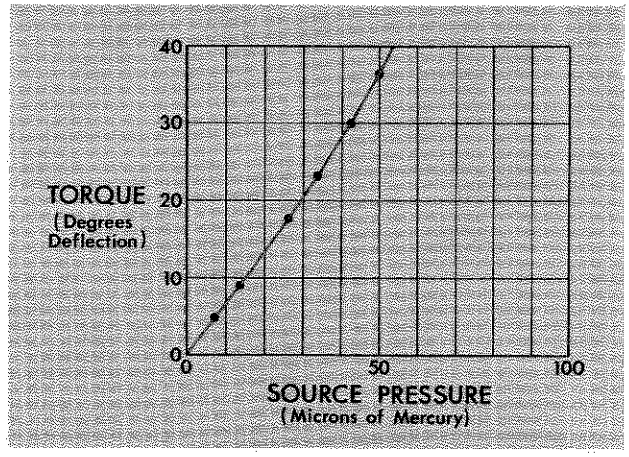

8. Typical results of momentum-transfer experiment of Fig. 7. For free molecular effusion from the source (up to about 30 microns of mercury), torque is proportional to source pressure. (Data points shown in the film were misplotted. Collisional effects near the source aperture cause the torque to increase at higher source pressures, as shown here.)

plotted versus source pressure. The departure from linearity at high pressures is due to departures from free-molecule flow in the vicinity of the source slit at high pressures.

Next, with source pressure held constant, the temperature of the target is increased by radiant heat transfer from a 1000-watt projection lamp. The resulting deflection of the target is like that produced by an increase in source pressure, because of the increased recoil momentum of molecules re-emitted from the hotter target.

The results of a series of experiments[2] of this type are shown in Fig. 9. Beams of various gases have exchanged momentum with an aluminum target over a range of target temperatures. The theoretical torque for the case in which the gas molecules are re-emitted

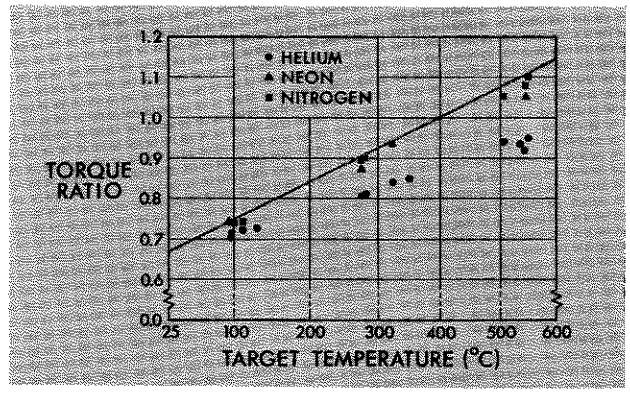

9. Increasing the target temperature (with source pressure held constant) causes an increase in the recoil momentum of the reflected molecules. Experimental results for nitrogen lie closer to the theoretical line for perfect accommodation than do the results for the helium and neon.

from the target as though they came out of a gas at equilibrium at the target temperature is shown as the solid line. This is called the case of *complete accommodation* of the re-emitted molecules to the target temperature. The experimental results for nitrogen lie close to this line, while those for helium and neon do not.

Mean Free Path as the Characteristic Length for Shock-Wave Structure

The shock wave in front of a model in a continuum hypersonic flow is examined in the wind tunnel shown in Fig. 10. The experiment also teaches something about heat transfer in rarefied flow.*

The model is a flat bar of aluminum mounted on a thin-walled stainless steel tube to reduce heat conduction to the wind-tunnel shell. It is placed in a free jet of air where the Mach number is approximately seven. The flow is made visible by the fluorescence excited in air by a beam of electrons which is passed across the flow well upstream of the model.**

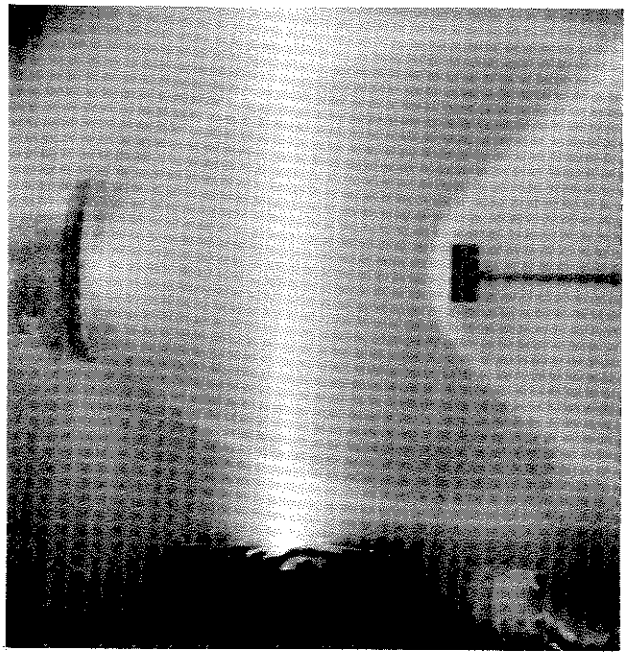

10. Flow from the freely expanding jet at the left is visualized by fluorescent excitement by an electron beam at right angles to the flow (center). A bow shock wave is seen in front of the sting-mounted object at the right.

In the experiment the structure of the shock wave is indicated by the varying recovery temperature of a fine thermocouple wire which is traversed through the shock wave. The wire is small enough to be always in free molecule flow, and does not disturb the shock wave by its presence. Figure 11 shows the wire temperature being plotted by an *x-y* recorder for a flow stagnation

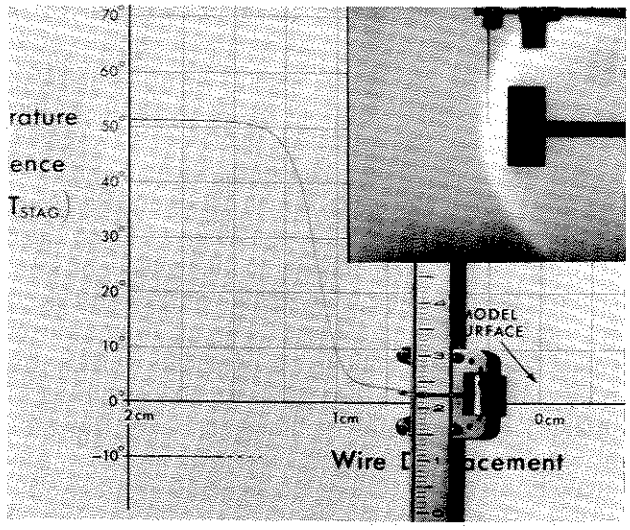

11. Wire temperature is plotted versus displacement as the thermocouple wire is traversed through the bow shock wave in front of the model (insert).

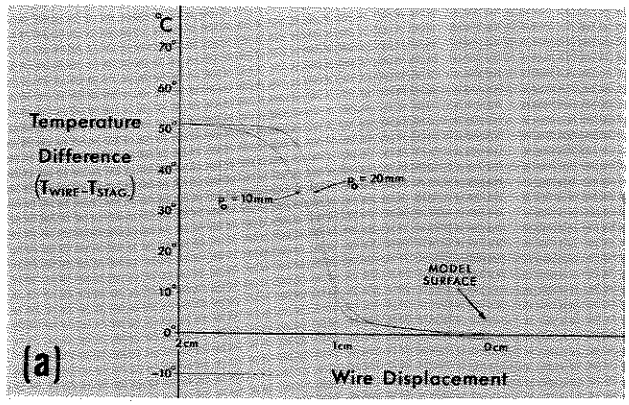

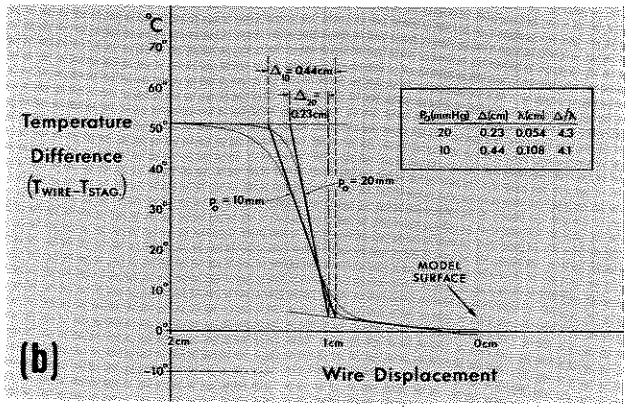

12. Comparison of the shock-wave profiles at stagnation pressures of 20 mm of Hg (20 torr) and 10 mm of Hg. (b) Determination of shock-wave thickness from asymptotes and tangents to the profiles. Results in table at upper right show that shock thickness is inversely proportional to the pressure, and hence proportional to the mean free path.

* The idea for the experiment comes from Sherman (1955),[3] who gives theoretical details of the wire-temperature interpretation at points within the shock wave, and empirical data on how small the wire must be.

** Because the fluorescence excited by the electron beam[4] is rather dim, each frame of the pictures showing the wire moving through the shock required an exposure of about 15 seconds.

pressure of 20 torr. Also shown in the insert are the model, shock wave, and wire supports.

Figures 12a and 12b show the temperature traces for stagnation pressures of 20 torr and 10 torr, and the shock thicknesses deduced from these traces. When the radius of curvature of the shock wave is much greater than the shock thickness, the mean free path is the only physical length to which the shock thickness can be proportional. The experiment confirms this proportionality and shows that the factor of proportionality is about 4 in air at Mach number 7.

Notice that when the wire is in the undisturbed flow upstream of the shock wave, it is much hotter than the model. The essential difference between wire and model is that Kn = 20 for the wire, while Kn = 0.03 for the model. This decrease in equilibrium temperature with decreasing Knudsen number is directly connected with the collisions between back-scattered molecules and those of the jet, and accompanies the formation of a shock wave.

References

1. **Vali, W., and Thomas, G. M. (1963), AIAA J. *1*, 2, 469-471.**
2. **Stickney, R. E., and Hurlbut, F. C. (1963), "Rarefied Gas Dynamics" J. A. Laurmann, editor, Vol. 1, 454-469, Academic Press.**
3. **Sherman, F. S. (1955), NACA TN 3298.**
4. **Muntz, E. P., and Marsden, D. J. (1963), "Rarefied Gas Dynamics" J. A. Laurmann, editor, Academic Press, Vol. II, 495-526.**